SIAM J. APPL. MATH.
Vol. 54, No. 5, pp. 1402–1424, October 1994

012

STABILITY AND BIFURCATIONS OF EQUILIBRIA IN A MULTIPLE-DELAYED DIFFERENTIAL EQUATION*

JACQUES BÉLAIR† AND SUE ANN CAMPBELL†

Abstract. The influence of multiple negative delayed feedback loops on the stability of a single-action mechanism are considered. A characteristic equation for the linearized stability of the equilibrium is completely analyzed, as a function of two parameters describing a delay in one loop and a ratio of the gains in the two feedback loops. The bifurcations occurring as the linear stability is lost are analyzed by the construction of a centre manifold. In particular, the nature of Hopf and more degenerate, higher codimension bifurcations are explicitly determined.

Key words. functional differential equations, feedback, Hopf bifurcations, normal forms

AMS subject classifications. 34K15, 58F36, 92C20

1. Introduction. Many biological and physical systems involving feedback mechanisms incorporate delays in their actions. This is particularly noteworthy in the regulation of physiological functions: the time required for a cell to mature, the time for the nerve impulse to travel along the axon and across the synapse, or the time for the hormonal signals to travel from their site of production to target organs by diffusion and/or passage through the circulation are but a few examples of such delays.

In this paper, we consider a delay-differential equation arising in a second attempt to understand the behavior of subjects trying to perform a "simple" motor control task (see [3] for a first attempt, and [2] for more details on this model). We study the equation

$$\dot{x}(t) = f_1(x(t - T_1)) + f_2(x(t - T_2)), \tag{1.1}$$

where $f_i(u) = -A_i \tanh(u), \quad i = 1, 2$ (A_i are positive constants), and first determine the asymptotic stability of the (unique) equilibrium solution $x = 0$. As long as we are only looking at the local (linearized) stability, it matters little what the actual functions f_i are, whenever their first derivatives at the origin are both negative. To determine the nature of a Hopf bifurcation (if any), however, we need derivatives of higher orders, and we thus have to use particular forms for the functions.

Computing $f_i'(0) = -A_i, \quad i = 1, 2$, and substituting, as is usual, $x(t) = e^{\lambda t}$ in (1.1) we obtain the characteristic equation

$$\lambda = -A_1 e^{-\lambda T_1} - A_2 e^{-\lambda T_2}. \tag{1.2}$$

By scaling the time in (1.1), it is possible to let one of the delays be equal to unity: we then have to investigate an equation in which only the *ratio* of the original delays appear. We do not consider this entirely appropriate in our context, however, since there is a significant loss of simplicity in the analysis using this normalization (more

* Received by the editors May 14, 1993; accepted for publication (in revised form) December 15, 1993. This work was supported by Natural Sciences and Engineering Research Council of Canada, Formation de chercheurs et aide á la recherche, Quebec, Fonds de Développement de la Recherche (Université de Montréal) and the North Atlantic Treaty Organization.

† Département de mathématiques et de statistique and Centre de recherches mathématiques, Université de Montréal, C.P. 6128-A, Montréal, Québec, H3C 3J7 and Centre for Nonlinear Dynamics in Physiology and Medicine, McGill University, Montreal, Quebec H3G 1Y6.

precisely, there are nontrivial complications in the determination of the full stability regions when this particular scaling is employed).

By scaling the variable $x(t)$, it is possible to let either one of the coefficients A_i be equal to unity in (1.1), to obtain the (normalized) characteristic equation

$$\lambda = -e^{-\lambda\tau_1} - Ae^{-\lambda\tau_2}, \tag{1.3}$$

where, in terms of the original parameters of (1.1), $t = A_1 t$, $\tau_i = A_1 T_i$ and $A = A_2/A_1$. Equation (1.3) now contains the three parameters A, τ_1, and τ_2. We can thus completely determine the region of stability in a two-parameter space by fixing the value of the remaining parameter, as has been accomplished recently in a similar problem [1].

For the current situation, there are three possible choices for the parameter to be fixed. We chose to fix τ_1 and consider the stability regions in the parameter plane (A, τ_2). This approach appears most natural to us in the context of modeling regulatory systems with multiple delayed feedback loops: given one such loop containing a time delay τ_1, the parameters A and τ_2 can be interpreted as the gain and the delay in an additional loop added to the original system. With this interpretation in mind, we concentrate our analysis on the values of A such that $|A| \leq 1$. By taking $A \geq 0$, the first part of the analysis will hold for the general case of negative feedback loops.

In the next section, we present a detailed analysis of the linear stability of (1.1). Nonlinear terms are considered in §3, at parameter values where one (in §3.1) or two (in §3.2) pairs of purely imaginary eigenvalues exist: possible secondary bifurcations are discussed, and numerical simulations illustrating them are presented. Related work is discussed in §4, where we compare our analysis with alternative ones recently used in the literature.

Our results are neither the most elegant nor the most general ones that can be obtained about (1.1). They are applicable to a specific system, however, and illustrate remarkably both the difficulties arising in the investigation of delay differential equations with multiple time delays, and how some of them can be overcome.

The problem we address is intrinsically multidimensional: scale changes reduce it to at best a three-parameter problem. Our analysis is one more illustration that "... a two-parameter problem is very different from a one-parameter problem" [9].

2. Local analysis. In this section, we determine, at a fixed value of τ_1, the values of the parameters A and τ_2 for which all roots of (1.3) satisfy $\mathrm{Re}(\lambda) < 0$. We consider mainly the value of A in the interval $[0, 1]$, for the reasons given in the previous section. We employ a previously successful version of the method of D subdivision [13].

The case when $\tau_1 = 0$ is well understood, being a particular case of a result of Hayes [12]. The technical motivation for the calculations of this section rely on the following basic Lemma, which generalizes one found in [5], both of which are special cases of a much more general result [8]. It is presented here for reasons of completeness.

LEMMA 2.1. *Consider the function* $g(\lambda, \tau) = \lambda + \sum_{j=1}^{m} a_j e^{-\tau_j \lambda}$, *where* a_j *are real numbers, and* $\tau_j \geq 0, 1 \leq j \leq m$. *Then as the value of any one of the numbers* τ_j *is varied, the number of zeros of the function* $g(\lambda, \tau)$ *with* $\mathrm{Re}(\lambda) > 0$, *counting multiplicities, can change only by a passage of* λ *through the imaginary axis.*

Proof. Denote $\lambda = \lambda(\tau)$ a solution of the equation $g(\lambda, \tau) = 0$ such that $0 < \mathrm{Re}(\lambda) < \infty$. Since $\lambda(u)$ is an analytic function of u, Rouché's theorem implies that there exists an $\epsilon > 0$ such that for $|U - T| < \epsilon$, there exists a root $\lambda(T)$, of the same multiplicity as $\lambda(U)$. Denote by $M(U)$ the total multiplicity of zeros in the open

right half plane, and suppose that $M(U)$ changes without a root appearing on the imaginary axis: this can only occur if there is a root at infinity, in which case there exists $\widetilde{U}$ and a sequence $\{U^{(i)}\}$ such that

$$\lim_{i\to\infty} U^{(i)} = \widetilde{U} \text{ and } \lim_{i\to\infty} |\lambda(U^{(i)})| = \infty, \tag{2.1}$$

where $|\ \ |$ denotes complex modulus, with $\mathrm{Re}(\lambda(U^{(i)}) \geq 0$. Then, since, for $1 \leq j \leq m$, $|e^{-\tau_j \lambda(.)}| \leq 1$,

$$\frac{g(\lambda,\tau)}{\lambda} = 1 + \sum_{j=1}^{m} a_j \lambda^{-1} e^{-\tau_j \lambda} \tag{2.2}$$

and thus $|g(\lambda,\tau)/\lambda| \to 1$ as $|\lambda| \to \infty$, contradicting $g(\lambda,\tau) = 0$. □

Remark. It is apparent from the proof of this Lemma that a similar result holds, for advanced equations ($\tau_j \leq 0$), to describe the crossing of eigenvalues in the left half plane.

From this last lemma, because it is applicable to (1.3), we can delineate the boundaries of the stability regions in the plane of the parameters as being those values for which there exists a purely imaginary root $\lambda = i\omega$ (including $\omega = 0$). It is thus essential to identify some region in which all the roots of eq.(1.3) have negative real parts. This is the content of the following

LEMMA 2.2. *Assume that, in* (1.3), $0 \leq A < 1$ *and* $0 \leq \tau_1 < \frac{1}{2}$; *then all solutions* λ *of* (1.3) *satisfy* $\mathrm{Re}(\lambda) < 0$.

Proof. Since $A \geq 0$, it is clear that (1.3) has no positive real root. Letting $\lambda = \mu + i\omega$ and separating real and imaginary parts of the resulting equation, we obtain

$$\mu = -e^{-\mu\tau_1}\cos\omega\tau_1 - Ae^{-\mu\tau_2}\cos\omega\tau_2, \tag{2.3a}$$

$$\omega = e^{-\mu\tau_1}\sin\omega\tau_1 + Ae^{-\mu\tau_2}\sin\omega\tau_2. \tag{2.3b}$$

Assume that (2.3) have roots μ and ω such that $\omega > 0$ (without loss of generality since complex roots of (1.3) come in complex conjugate pairs), and $\mu > 0$. It is obvious from (2.3a) that, since $A < 1$, $\mu < 2$; it is equally clear from (2.3b) that $\omega < 2$. In view of $\tau_1 < \frac{1}{2}$, we have $0 < \omega < 2 < 1/\tau_1$ and therefore $0 < \tau_1\omega < 1$, so that $0 < \cos 1 \leq \cos\omega\tau_1$ and $0 < \sin\omega\tau_1 \leq \sin 1$.

Write (2.3a) as $\mu + e^{-\mu\tau_1}\cos\omega\tau_1 = -Ae^{-\mu\tau_2}\cos\omega\tau_2$. Since $\cos\omega\tau_1 > 0$, it follows that $\cos\omega\tau_2 < 0$, and thus that $\mu < 1$. Isolating the last terms in the right hand side of each of (2.3a) and (2.3b), squaring the resulting equations and then adding them yields the necessary condition

$$A^2 = e^{2\mu\tau_2}[e^{-2\mu\tau_1} + \mu^2 + \omega^2 + 2e^{-\mu\tau_1}(\mu\cos\omega\tau_1 - \omega\sin\omega\tau_1)] \tag{2.4}$$

for a solution of (2.3) to exist. For fixed values of ω, τ_1 and τ_2, call $M(\mu)$ the right-hand side of the last equation. Since $\tau_1 < \frac{1}{2}$, it is clear that $M(0) \geq 1$. Compute the derivative $M'(\mu)$ as

$$\begin{aligned}\frac{dM}{d\mu} = {} & 2e^{2\mu\tau_2}[\mu^2\tau_2 + \mu + 2\mu\tau_2 e^{-\mu\tau_1}\cos\omega\tau_1 + \tau_2\omega(\omega - 2e^{-\mu\tau_1}\sin\omega\tau_1) \\ & + e^{-\mu\tau_1}((1-\tau_1\mu)\cos\omega\tau_1 + \omega\tau_1\sin\omega\tau_1) + (\tau_2 - \tau_1)e^{-2\mu\tau_1}].\end{aligned} \tag{2.5}$$

It is obvious that $M'(0) = 2[\tau_2\omega(\omega - 2\sin\omega\tau_1) + (\cos\omega\tau_1 + \omega\tau_1\sin\omega\tau_1) + \tau_2 - \tau_1] > 0$, since $\tau_1 < \frac{1}{2} < \cos(1) \leq \cos\omega\tau_1$. We have $(1-\tau_1\mu)\cos\omega\tau_1 + \omega\tau_1\sin\omega\tau_1 + (\tau_2 -$

$\tau_1)e^{-\mu\tau_1} \geq (1-\tau_1)\cos\omega\tau_1 + \omega\tau_1 \sin\omega\tau_1 + (\tau_2-\tau_1)e^{-\mu\tau_1} \equiv N(\mu)$. Define the auxiliary function $h(x) = x\sin x + (1-\tau_1)\cos x$, so that $h'(x) = x\cos x + \tau_1 \sin x$ and thus $h'(0) = 0$. For $0 < x \leq 1$, it is not difficult to show that both $h(x)$ and $h'(x)$ are positive-valued, so that $h(x) \geq h(0) > \tau_1 > \tau_1 e^{-\mu\tau_1}$. It is thus clear that $\frac{dM}{d\mu}$ is always positive when μ is nonnegative and so there can be no root of (2.3) when $A < 1$. □

THEOREM 2.3. *The values of the parameters A and τ_2 for which* (1.3) *has a root with zero real part are given by*

$$A = \sqrt{1+\omega^2 - 2\omega\sin\omega\tau_1} = \sqrt{\cos^2\omega\tau_1 + (\omega - \sin\omega\tau_1)^2} \quad \textit{and} \tag{2.6a}$$

$$\tau_2 = \frac{\arctan\left[\frac{\sin\omega\tau_1 - \omega}{\cos\omega\tau_1}\right]}{\omega}. \tag{2.6b}$$

Proof. Since A is nonnegative, it is clear that (1.3) can have no real positive solution. Let $\mu = 0$ in (2.3) so that λ is a purely imaginary root $i\omega$ of (1.3), and write these equations as

$$\cos\omega\tau_1 = -A\cos\omega\tau_2, \tag{2.7a}$$

$$\omega - \sin\omega\tau_1 = A\sin\omega\tau_2. \tag{2.7b}$$

Squaring each side of both of these last equations and adding yields (2.6a). Dividing (2.7b) by (2.7a) in turn gives

$$\tan(\omega\tau_2) = \frac{\sin\omega\tau_1 - \omega}{\cos\omega\tau_1}, \tag{2.8}$$

from which (2.6b) follows. □

With the boundaries of the stability region given by the "simple" (2.6), it remains to determine which branches of the inverse tangent functions must be taken in (2.6b), and how the imaginary roots change as the parameters A and τ_2 are varied. For this, we have to study in detail each of the expressions defined by (2.6), as a function of ω.

From (2.6a) it is clear that

$$\frac{dA}{d\omega} = [\omega - \omega\tau_1\cos(\omega\tau_1) - \sin(\omega\tau_1)]/A. \tag{2.9}$$

By differentiating each member of (1.3) with respect to τ_2, all the other parameters staying constant, we obtain

$$\frac{d\lambda}{d\tau_2} = \frac{A\lambda e^{-\lambda\tau_2}}{1 - \tau_1 e^{-\lambda\tau_1} - A\tau_2 e^{-\lambda\tau_2}}, \tag{2.10}$$

which yields, when evaluated at a purely imaginary value $\lambda = i\omega$, after using (2.7) and taking the real part of the ensuing equality,

$$\frac{d\mathrm{Re}\lambda}{d\tau_2} = \frac{\omega(\omega - \omega\tau_1\cos(\omega\tau_1) - \sin(\omega\tau_1))}{[1 + (\tau_2 - \tau_1)\cos(\omega\tau_1)]^2 + [\omega\tau_2 - (\tau_2 - \tau_1)\sin(\omega\tau_1)]^2}. \tag{2.11}$$

From this, we readily obtain

LEMMA 2.4. *The eigenvalues λ of* (1.3) *enter the right-half of the complex plane when τ_2 increases and crosses one branch of the curve defined by equations* (2.6) *along which A is increasing as a function of ω.*

Proof. From (2.9) and (2.11), it follows that when $A(\omega)$ is increasing along a curve defined by (2.6), a purely imaginary eigenvalue moves from the left-half to the right-half of the complex plane, when τ_2 is increased (and vice-versa). □

Consider, at a fixed value of τ_1, the function $f(\omega) = (\sin\omega\tau_1 - \omega)/\cos\omega\tau_1$, the right-hand side of (2.8), which we also write as $f_1(\omega)/\cos\omega\tau_1$. It is not too difficult to see, from (2.9) that the function A is monotone increasing when $\tau_1 < 1/2$: this follows most easily, remembering that τ_1 is fixed, from a comparison of the functions $f_1(\omega)$ and $g(\omega) = \omega\tau_1\cos(\omega\tau_1)$.

It is also clear that when $\tau_1 > 1/2$, the function $A(\omega)$ can be either decreasing or increasing (in ω), since it has extrema at all roots of $g(\omega) = -f_1(\omega)$. (For use in Theorem 2.7, denote by a_0 the value of A at such a root, in the interval $(0, \pi/\tau_1)$.)

To study the function defining τ_2 by (2.6b), let us first denote, for a positive integer j, by r_j the solution $r = r_j \in (2\pi j, (4j+1)\pi/2)$ of the transcendental equation $r = \tan r$.

LEMMA 2.5. *For a fixed positive value of τ_1, the function $f_1(\omega) = \sin\omega\tau_1 - \omega$ is negative for $\omega > 1$, and has a finite (possibly zero) number of sign changes for ω in the interval $[0,1]$. This number of sign changes is modified (and increases with increasing τ_1) when τ_1 has a value $\sqrt{1+r^2}$, where $r = r_j$ (j any positive integer).*

Proof. The first statement is obvious. The sign changes in f_1 are best seen by considering fixed, successively increasing values of the parameter τ_1.

Comparing the graphs of $\sin\omega\tau_1$ and ω reveals that

(i) for $\tau_1 < 1$, $\sin\omega\tau_1 < \omega$ for all values of ω;

(ii) for $1 < \tau_1 < \pi/2$, $f_1(\omega)$ is positive when $\omega \in (0, \omega_1)$, where $\omega_1 \in (0, \pi/2\tau_1)$ is defined as the solution of $\omega_1 = \sin\omega_1\tau_1$, and $f_1(\omega) > 0$ for $\omega > \omega_1$;

(iii) an additional (pair of) root(s) of $\sin\omega\tau_1 = \omega$ appear(s) in the interval $(2\pi/\tau_1, 5\pi/2\tau_1)$, when the straight line ω is tangent to the function $\sin\omega\tau_1$: this means that both equations $\sin\omega\tau_1 = \omega$ and $\tau_1\cos\omega\tau_1 = 1$ are simultaneously satisfied, which is equivalent to $\tan\omega\tau_1 = \omega\tau_1$. Thus when $\omega\tau_1 = r_1$ satisfies $r = \tan r$, $\tau_1 = \sqrt{1+r_1^2}$. It is equally clear that for $\sqrt{1+r_1^2} < \tau_1 < 5\pi/2$, there are two roots ω_2 and ω_3 in $(2\pi/\tau_1, 5\pi/2\tau_1)$ satisfying $\sin\omega_i\tau_1 = \omega_i$ $(i = 2,3)$, that $\omega_3 = 1$ when $\tau_1 = 5\pi/2$ and that for all $\tau_1 > 5\pi/2$, $\omega_2 \in (2\pi/\tau_1, 5\pi/2\tau_1)$ and $\omega_3 \in (5\pi/2\tau_1, 3\pi/\tau_1)$;

(iv) as τ_1 increases further, two new roots of $\sin\omega\tau_1 = \omega$ appear when τ_1 reaches a value $\sqrt{1+r_j^2}$, these roots are in the interval $(2j\pi/\tau_1, (4j+1)\pi/2\tau_1)$ for $\sqrt{1+r_j^2} < \tau_1 < (4j+1)\pi/2$ and for $\tau_1 > (4j+1)\pi/2$, there is one root ω_{2j} in $(2j\pi/\tau_1, (4j+1)\pi/2\tau_1)$, and another root ω_{2j+1} in $((4j+1)\pi/2\tau_1, (2j+1)\pi/\tau_1)$. Obviously, the zeros of the function f coincide with those of the function $f_1(\omega)$, and the poles of $f(\omega)$ are located precisely at the zeros of $\cos\omega\tau_1$. □

When $\tau_1 < 1$, the function f therefore only possesses poles. Since $f(0) = 0$, and $f'(0) = \tau_1 - 1$, $f(\omega)$ will be monotone decreasing when ω is between 0 and $\pi/2\tau_1$. In each interval $((2j+1)\pi/2\tau_1, (2j+3)\pi/2\tau_1)$ (j a positive integer), $f(\omega)$ has a unique extremum (a maximum for even values of j and a minimum for odd values of j), and its value at these extrema is monotonically and unboundedly increasing (in absolute value). More generally, when $\tau_1 > 1$, and for each value of τ_1, we can precisely describe the behaviour of the function f: it suffices to consider the successive occurrence on the ω positive axis, of the poles and zeros of the function $f(\omega)$, as summarized in the following.

LEMMA 2.6. *Assume that $1 < \tau_1$ is fixed, and recall the definitions given above of r_j and ω_l (j and l positive integers). Then, as a function of ω, according to the value of τ_1, the function $f(\omega)$ is*

(i) $\tau_1 < \pi/2$: *positive and continuous for* $\omega \in (0, \omega_1)$, *negative and continuous for* $\omega \in (\omega_1, \pi/2\tau_1)$, *and successively positive and negative for* ω *in each interval* $(k\pi/2\tau_1, (k+2)\pi/2\tau_1)$, k *an odd integer, with a pole at the endpoints of each of the intervals and no zeros in their interiors*;

(ii) $\pi/2 < \tau_1 < \sqrt{1+r_1^2}$: *positive and continuous for* $\omega \in (0, \pi/2\tau_1)$, *monotonically increasing from* $-\infty$ *to* ∞ *for* $\omega \in (\pi/2\tau_1, 3\pi/2\tau_1)$, *and successively negative and positive for* ω *in each interval* $(k\pi/2\tau_1, (k+2)\pi/2\tau_1)$, $3 \le k$ *an odd positive integer, with a pole at the endpoints of each of the intervals and no zeros in their interiors*;

(iii) $\sqrt{1+r_1^2} < \tau_1 < 5\pi/2$: *positive and continuous for* $\omega \in (0, \pi/2\tau_1)$, *monotonically increasing from* $-\infty$ *to* ∞ *for* $\omega \in (\pi/2\tau_1, 3\pi/2\tau_1)$, *negative and continuous for* $\omega \in (3\pi/2\tau_1, \omega_2)$, *positive for* $\omega \in (\omega_2, \omega_3)$, *and continuously decreasing from* 0 *to* $-\infty$ *for* $\omega \in (\omega_3, 5\pi/2\tau_1)$, *and successively positive and negative for* ω *in each interval* $(k\pi/2\tau_1, (k+2)\pi/2\tau_1)$, $5 \le k$ *an odd integer, with a pole at the endpoints of each of the intervals and no zeros in their interiors*;

(iv) $\tau_1 \in ((4p-3)\pi/2, \sqrt{1+r_p^2})$, *with* p *a positive integer: monotonically increasing on each of the intervals* $(0, \pi/2\tau_1)$ *and* $(k\pi/2\tau_1, (k+2)\pi/2\tau_1)$, $k = 1, \dots, p-1$, *and successively negative and positive for* ω *in each interval* $(k\pi/2\tau_1, (k+2)\pi/2\tau_1)$, $p+1 \le k$ *an odd positive integer, with a pole at the endpoints of each of the intervals and no zeros in their interiors*;

(v) $\tau_1 \in (\sqrt{1+r_p^2}, (4p+1)\pi/2)$, *with* p *a positive integer*: *monotonically increasing on each of the intervals* $(0, \pi/2\tau_1)$ *and* $(k\pi/2\tau_1, (k+2)\pi/2\tau_1)$, $k = 1, \dots, p-1$, *negative and continuous for* $\omega \in ((p+1)\pi/2\tau_1, \omega_{2p})$, *positive for* $\omega \in (\omega_{2p}, \omega_{2p+1})$, *and continuously decreasing from* 0 *to* $-\infty$ *for* $\omega \in (\omega_{2p+1}, (p+2)\pi/2\tau_1)$, *and successively positive and negative for* ω *in each interval* $(n\pi/2\tau_1, (n+2)\pi/2\tau_1)$, $p+2 \le n$ *an odd integer, with a pole at the endpoints of each of the intervals and no zeros in their interiors.*

Since the parameter A is positive-valued, (2.7a) implies that the functions $\cos\omega\tau_1$ and $\cos\omega\tau_2$ must be of opposite signs, and (2.7b) forces the functions $\omega - \sin\omega\tau_1$ and $\sin\omega\tau_2$ to have the same sign. The signs of the functions $f(\omega)$, $\cos\omega\tau_1$ and $\sin\omega\tau_1$ are thus somewhat restricted for ω to be a root of (2.7). Therefore, from the two lemmas above, we can infer, with a_0 as defined just after Lemma 2.4, the following.

THEOREM 2.7. *For a fixed, positive value of* τ_1, *let*

$$T_j = \frac{\arctan\left[\frac{\sin\omega\tau_1 - \omega}{\cos\omega\tau_1}\right]}{\omega} \tag{2.12}$$

where the arctangent takes its value in the interval $(2\pi j, (2j+1)\pi)$. *Then the nonnegative values of the parameters* A *and* τ_2 *for which all roots of* (1.3) *satisfy* $\mathrm{Re}(\lambda) < 0$ *are given, according to the value of* τ_1, *by*:

(2.13)

$$\tau_1 < 1/2\text{: } A < 1, \quad \text{or} \quad A > 1 \quad \text{and} \quad \tau_2 < T_0;$$

$$1/2 < \tau_1 < \pi/2\text{: } A < a_0, \quad \text{or} \quad A > a_0 \quad \text{and} \quad \tau_2 < T_0 \quad \text{or} \quad T_{2p-1} < \tau_2 < T_{2p};$$

$$\pi/2 < \tau_1 < \sqrt{1+r_1^2}\text{: } 0 < \tau_2 < T_0, \quad \text{or} \quad T_{2p-1} < \tau_2 < T_{2p};$$

$$\sqrt{1+r_1^2} < \tau_1\text{: } 0 < \tau_2 < T_0,$$

where p *is any positive integer.*

The main results of the previous paragraphs are illustrated in Figs. 2.1–2.4, where the parameter values in the plane (A, τ_2) for which the null solution of (1.1) is linearly asymptotically stable are shown (in the hatched region). The boundary of each of these regions is given by the different branches of the curve defined by (2.6), for positive values of ω. In all cases, $\lim_{\omega\to 0} A(\omega) = 1$ and $\lim_{\omega\to\infty} A(\omega) = \infty$; also, for $\tau_1 < \pi/2$, $\lim_{\omega\to 0} \tau_2(\omega) = \infty$ and $\lim_{\omega\to\infty} \tau_2(\omega) = 0$ along all branches of the arctangents. The different curves are thus different paths joining the points $(1, \infty)$ and $(\infty, 0)$ in the plane of the parameters (A, τ_2).

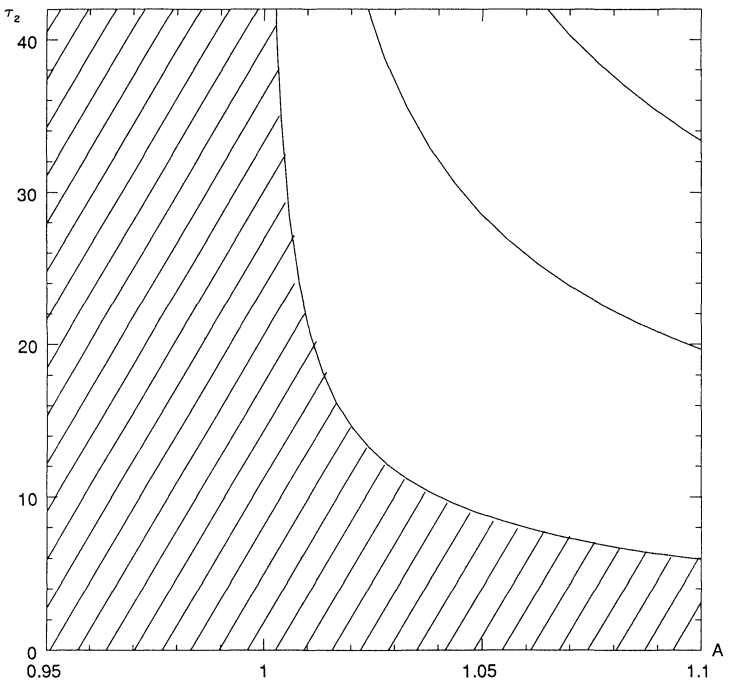

FIG. 2.1. *Region of stability for the null solution of* (1.1): *local asymptotic stability holds for parameter values in the hatched region. Here,* $\tau_1 = 0$, *but the diagram is qualitatively unchanged for* τ_1 *between* 0 *and* 1/2. *Solid lines indicate a supercritical Hopf bifurcation and are given by* (2.6).

The stability region is shown for $\tau_1 = 0$ in Fig. 2.1. For values of the gain $A > 1$, a sufficiently large delay τ_2 will destabilize the stationary solution; for values of A less (or equal) to 1, however, the steady state is always stable (i.e., for all values of A in this range and all positive values of τ_2).

When $0 \leq \tau_1 < 1/2$, the structure of the region of stability does not change qualitatively, although it quantitatively and continuously evolves: the convex curve representing, for $A > 1$, the upper bound τ_2 of the stability region is lowered as τ_1 increases.

A significant modification occurs (Fig. 2.2), however, when τ_1 becomes slightly greater than 1/2. The boundary of the stability region is now made up of infinitely many arcs of curves, given by (2.6) and associated with the different branches of the inverse tangent function of (2.6b). The most remarkable effects of this change are that (i) there are now values of $A < 1$ for which destabilization of the null solution can occur (so that a lower relative gain is needed in the second loop to induce oscillations) and (ii) as the delay τ_2 is increased, many stability switches may occur, for a fixed

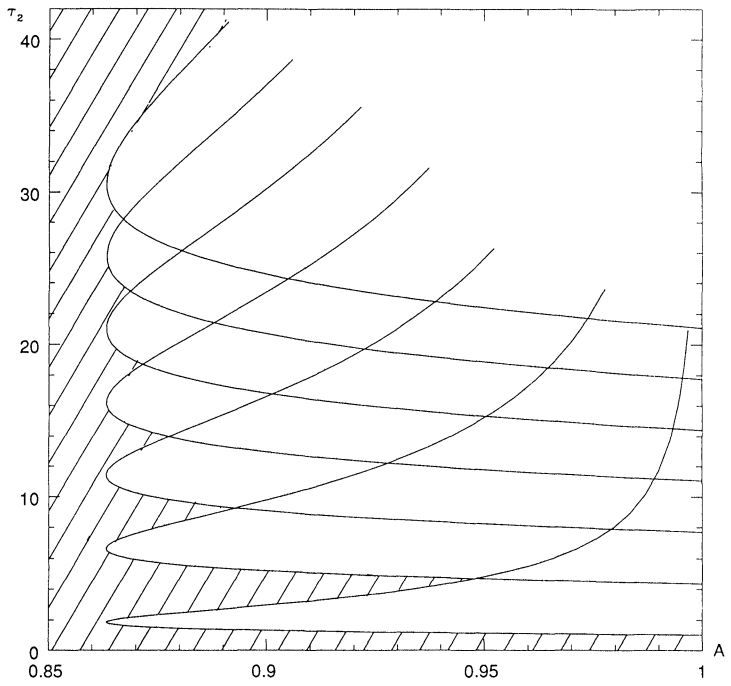

FIG. 2.2. *Same as in Fig.* 2.1, *except now* $\tau_1 = 0.65$; *the diagram is qualitatively unchanged for* τ_1 *between* $1/2$ *and* $\pi/2$.

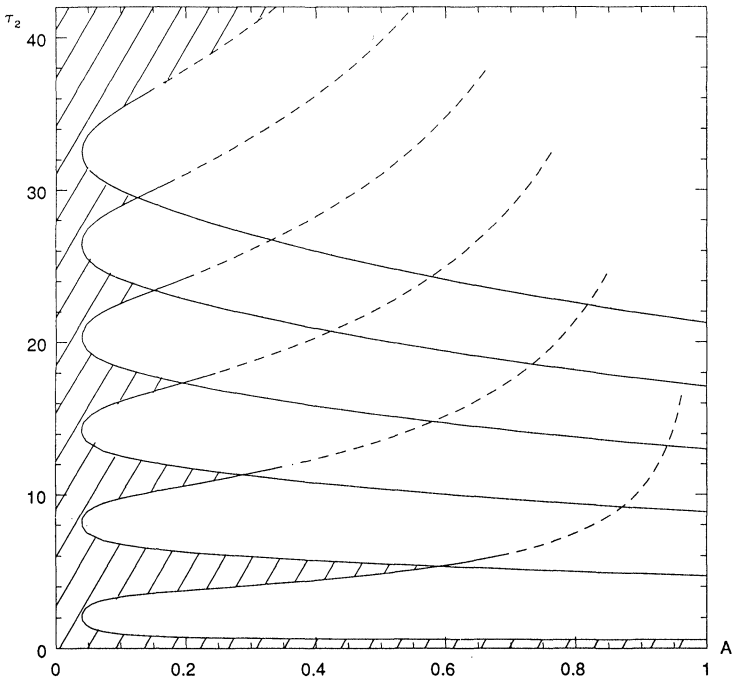

FIG. 2.3. *Same as in Fig.* 2.1, *except now* $\tau_1 = 1.5$; *the diagram is qualitatively unchanged for* τ_1 *between* $1/2$ *and* $\pi/2$. *Solid lines indicate the Hopf bifurcation is supercritical, dashed lines indicate it is subcritical, according to the sign of* a *in* (3.21).

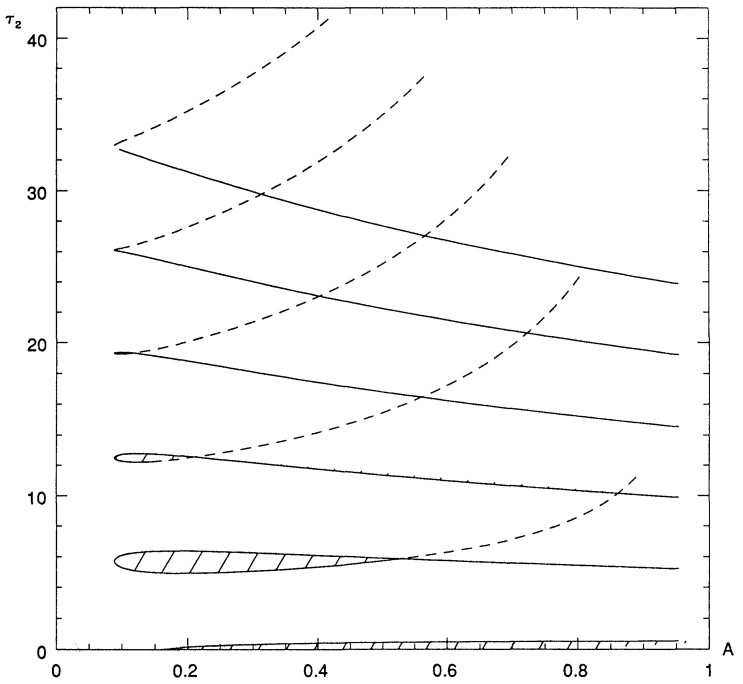

FIG. 2.4. *Same as in Fig.* 2.1, *except now* $\tau_1 = 1.75$*; the diagram is qualitatively unchanged for* τ_1 *between* $\pi/2$ *and* $\sqrt{1+r_1^2}$ *where* r_1 *is defined in* §2. *Solid lines indicate the Hopf bifurcation is supercritical, dashed lines indicate it is subcritical, according to the sign of* a *in* (3.21). *Notice that the stability region is now multiply connected.*

value of the gain A (< 1). This is in sharp contrast with the previous ($\tau_1 < 1/2$) case, where increasing either τ_2 or A lead to a destabilization, but further increases could not induce restabilization of the stationary solution.

When τ_1 is increased past the value $\pi/2$, another significant change of the region of asymptotic stability takes place: it is substantially reduced in area, and it becomes multiply connected, as shown in Fig. 2.4. There are now values of A (those smaller than $-\cos\omega\tau_1$, where ω is the smallest positive root of $\omega = \sin\omega\tau_1$) for which the null solution of (1.1) is unstable for arbitrarily low values of τ_2. For all other values of A, this stationary solution can always be stabilized by decreasing the value of τ_2 and keeping A fixed. Contrary to the previous cases, decreasing the value of A cannot always restabilize the null steady state. These strategies of how to restabilize an otherwise unstable equilibrium have been discussed in the context of modeling motor control [2].

A noticeable consequence of the changes occurring when τ_1 is greater than $1/2$ is that there are parameter values of A and τ_2 for which two pairs of imaginary (complex conjugate) eigenvalues coexist. These correspond to the coincidence of fixed but particular values of A and τ_2, from (2.6) for two different values of ω. This coincidence requires the nonmonotonicity of A as a function of ω, and also the multiplicity of the inverse trigonometric function defining τ_2. These degenerate points will be further discussed in the next section.

We have described in detail the parameter values at which, and the mechanism by which, in the plane of the parameters (A, τ_2), (1.3) acquires one or more roots

with positive real parts. In the least degenerate case, a Hopf bifurcation may take place as the stability of the null solution of (1.1) is lost. The determination of the exact nature of this bifurcation (for example, whether it is degenerate, subcritical or supercritical) entails nontrivial computations, even for delay-differential equations much simpler than the one studied here: among other things, higher-order terms of the Taylor expansions of the functions f_i of (1.1) must be taken into account. These computations are done on a specific (but motivated [2]) example in the next section.

3. Centre manifold analysis. We consider a general differential delay equation expressed, in standard notation [8] as a functional differential equation

$$\dot{x} = Lx_t + f(x_t), \tag{3.1}$$

with $x_t = x(t+\theta)$, $-h \le \theta \le 0$, $C = C([-h, 0], \mathbb{R})$, $L : C \to \mathbb{R}$ a linear operator, and $g \in C^r(C, \mathbb{R})$, $r \ge 1$. L may be expressed in integral form as

$$L\phi = \int_{-h}^{0} [d\eta(\theta)]\phi(\theta), \tag{3.2}$$

where $\eta : [-h, 0] \to \mathbb{R}$ is a function of bounded variation. We assume that any parameters in the model are such that the linear part of the equation

$$\dot{x}(t) = Lx_t \tag{3.3}$$

has m eigenvalues with zero real parts, all other eigenvalues having negative real parts. In such a situation, Hale [10] has shown that there exists in the state space C an m-dimensional invariant manifold, the centre manifold, and that long term behavior of solutions to the nonlinear equation is well approximated by the flow on this manifold. We outline the steps involved in calculating this manifold in the following paragraphs and then apply it to our equation in §§3.1–3.2.

At a point in parameter space where the linear equation (3.3) possesses m eigenvalues with zero real parts, there exists a splitting of the space $C = P \oplus Q$. P is an m-dimensional subspace spanned by the solutions to (3.3) corresponding to the m zero real part eigenvalues, and P and Q are invariant under the flow associated with eq.(3.3). Further, the centre manifold introduced above is given by

$$M_f = \{\phi \in C : \phi = \Phi\mathbf{z} + h(\mathbf{z}, f), \mathbf{z} \text{in a neighbourhood of zero in } \mathbb{R}^m\}.$$

The flow on this centre manifold is

$$x_t = \Phi\mathbf{z}(t) + h(\mathbf{z}(t), f), \tag{3.4}$$

where Φ is a basis for P, $h \in Q$, and $\mathbf{z}$ satisfies the ordinary differential equation

$$\dot{\mathbf{z}} = B\mathbf{z} + \mathbf{b}f(\Phi\mathbf{z}). \tag{3.5}$$

In (3.5), B is the $(m \times m)$ matrix of eigenvalues with null real part of (3.3), and $\mathbf{b}$ is determined from the solution to the equation adjoint to (3.1). Specifically, if we let Ψ be the basis for the invariant subspace of the adjoint problem corresponding to P, then $\mathbf{b} = \Psi(0)$, where Ψ is normalized by

$$\langle \Psi, \Phi \rangle = \mathrm{I}, \tag{3.6}$$

where I is the $m \times m$ identity matrix and

$$\langle \psi, \phi \rangle = \psi(0)\phi(0) - \int_{-h}^{0} \int_{0}^{\theta} \psi(\xi - \theta)[d\eta(\theta)]\phi(\xi)\, d\xi \tag{3.7}$$

is the bilinear form associated with (3.3). If we let the elements of Ψ be linear combinations of those of Φ, i.e., $\Psi = K\Phi^T$ (K an $m \times m$ matrix of constants), then $K = \langle \Phi^T, \Phi \rangle^{-1}$ or $\Psi = \langle \Phi^T, \Phi \rangle^{-1} \Phi$. Thus the problem of describing the long term behaviour of solutions to the delay differential (1.1) has been reduced (locally) to the problem of describing the behaviour of solutions to the m-dimensional system of ordinary differential equations (3.5).

Although straightforward in principle, the practical implementation of this procedure, especially in the case of a center manifold of dimension greater than 2, is far from trivial: we had to rely on the algebraic manipulation language MAPLE [18] to perform the calculations of §3.2. A description of the program with a *simple* illustration appears in [4]. Even then, simplifications based upon such relations as (2.7) must be explicitly used for the calculations to be accomplished on a computer with finite memory.

3.1. Single Hopf. We return to the full (1.1) with the scalings of §1 incorporated. Near the equilibrium $x(t) = 0$, the hyperbolic tangent may be expanded in a Taylor series giving

$$\begin{aligned} \dot{x}(t) &= -[x(t-\tau_1)) + Ax(t-\tau_2)] + \left[\frac{x^3(t-\tau_1)}{3} + A\frac{x^3(t-\tau_2)}{3}\right] \\ &\quad + O(x^5(t-\tau_1), x^5(t-\tau_2)) \\ &= Lx_t + f(x_t) + O(x_t^5), \end{aligned} \tag{3.8}$$

which defines our functional differential equation. We note that in the case of discrete delays the function $\eta(\theta)$ which expresses L as an integral operator is just the Dirac delta "function," i.e.,

$$x(t-\tau) = \int_{-\tau}^{0} \delta(\theta + \tau)x_t\, d\theta. \tag{3.9}$$

Section 2 analyzed in detail the location of the eigenvalues of the linearized equation showing the destabilization of the trivial solution through a Hopf bifurcation. On each branch of this Hopf bifurcation, there are two eigenvalues with zero real parts: $\pm i\omega$, where ω varies along the branch. To understand the behaviour of solutions near this bifurcation, and in particular to investigate the stability of the resulting periodic orbits, we need to include the effects of the nonlinear terms of the equation. We follow the procedure outlined above, calculating the centre manifold near an arbitrary Hopf bifurcation point as a function of ω. This accomplished, we may obtain the appropriate centre manifold for any given point on a branch of the Hopf bifurcation curve by simply substituting in the value of ω corresponding to the point.

In the case of the single Hopf bifurcation, there are two eigenvalues with zero real parts, and the elements needed to write (3.5) are

$$\begin{aligned} \Phi = (\phi_1, \phi_2) = (\sin(\omega\theta), \cos(\omega\theta)), \qquad \mathbf{z} = (x, y)^T, \\ \text{and thus} \qquad \Phi\mathbf{z} = \sin(\omega\theta)x + \cos(\omega\theta)y, \end{aligned} \tag{3.10}$$

$$B = \begin{bmatrix} 0 & -\omega \\ \omega & 0 \end{bmatrix}, \quad \text{and} \tag{3.11}$$

$$\mathbf{b} = \Psi(0) = \begin{pmatrix} K_{11}\phi_1(0) + K_{12}\phi_2(0) \\ K_{21}\phi_1(0) + K_{22}\phi_2(0) \end{pmatrix} = \frac{1}{\det \langle \Phi^T, \Phi \rangle} \begin{pmatrix} \langle \phi_2, \phi_1 \rangle \\ \langle \phi_2, \phi_2 \rangle \end{pmatrix}. \tag{3.12}$$

Using (3.9) we see that the inner product for the problem is

$$\langle \psi, \phi \rangle = \psi(0)\phi(0) - \int_{-\tau_1}^{0} \psi(\xi + \tau_1)\phi(\xi)\, d\xi - A \int_{-\tau_2}^{0} \psi(\xi + \tau_2)\phi(\xi)\, d\xi. \tag{3.13}$$

The elements of $\langle \Phi^T, \Phi \rangle$ may thus be calculated as functions of ω, so that

$$\begin{aligned} \langle \phi_1, \phi_1 \rangle = \langle \phi_2, \phi_2 \rangle &= \frac{1}{2}\left[1 + (\tau_2 - \tau_1)\cos(\omega\tau_1)\right], \\ \langle \phi_1, \phi_2 \rangle = -\langle \phi_2, \phi_1 \rangle &= \frac{1}{2}\left[-\omega\tau_2 + (\tau_2 - \tau_1)\sin(\omega\tau_1)\right]. \end{aligned} \tag{3.14}$$

The function f in (3.8) thus yields

$$\begin{aligned} f(\Phi z) &= \frac{1}{3}[-\sin(\omega\tau_1)x + \cos(\omega\tau_1)y]^3 + \frac{A}{3}[-\sin(\omega\tau_2)x + \cos(\omega\tau_2)y]^3 \\ &= f_{111}x^3 + f_{112}x^2y + f_{122}xy^2 + f_{222}y^3, \\ &\quad \text{where e.g. } f_{111} = -\frac{1}{3}\left[\sin^3(\omega\tau_1) + A\sin^3(\omega\tau_2)\right]. \end{aligned} \tag{3.15}$$

Substituting (3.10), (3.12), and (3.15) in (3.5) gives, for the dynamical system on the centre manifold, the explicit expression

$$\begin{aligned} \dot{x} &= -\omega y + F^1_{111}x^3 + F^1_{112}x^2y + F^1_{122}xy^2 + F^1_{222}y^3, \\ \dot{y} &= \omega x + F^2_{111}x^3 + F^2_{112}x^2y + F^2_{122}xy^2 + F^2_{222}y^3, \end{aligned} \tag{3.16}$$

where $F^j_{111} = b_j f_{111}$, etc. These equations can be simplified by a near-identity transformation, to the normal form, to third order [7, §3.3]

$$\begin{aligned} \dot{x} &= a(x^2 + y^2)x - (\omega + b(x^2 + y^2))y, \\ \dot{y} &= (\omega + b(x^2 + y^2))x + a(x^2 + y^2)y. \end{aligned} \tag{3.17}$$

Expressed in polar coordinates, this degenerate system becomes

$$\dot{r} = ar^3, \qquad \dot{\theta} = \omega + br^2 \tag{3.18}$$

and its unfolding is well known [7] to be

$$\dot{r} = \mu r + ar^3, \qquad \dot{\theta} = \omega + br^2, \tag{3.19}$$

where μ is an unfolding parameter. The rôle of this unfolding parameter is that *all* possible behaviors of systems close to (3.18) must be contained in a system of the form of (3.19). Analysis of these equations [7, §3.4] reveals that there are two distinct cases depending on the sign of the cubic coefficient a (see Fig. 3.1). If $a < 0$ then the Hopf bifurcation gives rise to a stable limit cycle and it is called supercritical; if

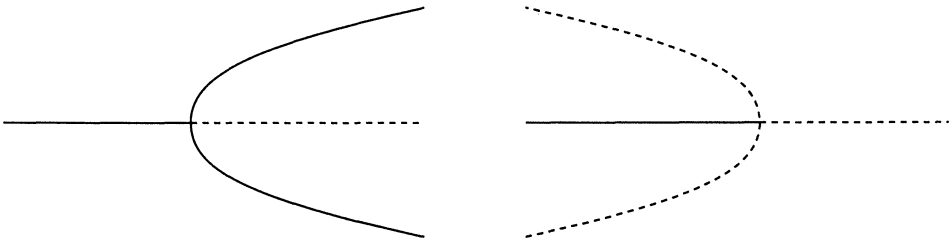

FIG. 3.1. *Criticality of a Hopf bifurcation, according to the sign of the a from* (3.21). *A solid line indicates stability of either the equilibrium point or the limit cycle, dashed line indicates instability of the same*: (a) *supercritical* ($a < 0$) (b) *subcritical* ($a > 0$). *The horizontal axis is a bifurcation parameter, the vertical coordinate is the amplitude of a limit cycle.*

$a > 0$, the bifurcation gives rise to an unstable limit cycle and is called subcritical. The coefficient a in these equations is given by

$$a = \frac{1}{8}\left[3F^1_{111} + F^1_{122} + F^2_{112} + 3F^2_{222}\right].$$

For our particular case, a may be given explicitly as a function of ω and the parameters of (3.15), namely,

$$\begin{aligned} a &= \frac{1}{8}\left[3b_1 f_{111} + b_1 f_{122} + b_2 f_{112} + 3b_2 f_{222}\right] \\ &= \frac{1}{8}\left\{-b_1\left[\sin(\omega\tau_1) + A\sin(\omega\tau_2)\right] + b_2[\cos(\omega\tau_1) + A\cos(\omega\tau_2)]\right\}. \end{aligned} \tag{3.20}$$

Using (2.7b),(3.12), and (3.14), this last equation can be further reduced to

$$a = \frac{-b_1\omega}{8} = \frac{-\omega}{8}\left[\frac{\langle\phi_2,\phi_1\rangle}{\det\langle\Phi^{\mathrm{T}},\Phi\rangle}\right] = \frac{\omega}{16D^2}\left[\tau_2(\sin(\omega\tau_1) - \omega) - \tau_1\sin(\omega\tau_1)\right], \tag{3.21}$$

which allows us to study the criticality of the bifurcation as a function of ω and the parameters. This leads to the following.

THEOREM 3.1. *For* $\tau_1 < 1$, *each branch of the Hopf bifurcation is everywhere supercritical.*

Proof. We need to show that $a(\omega) < 0$ for all ω on each branch of the Hopf bifurcation. On each branch, the sign of $a(\omega)$ will be determined by the sign of

$$h(\omega) = \tau_2[\sin(\omega\tau_1) - \omega] - \tau_1\sin(\omega\tau_1) = \tau_2 f_1(\omega) - \tau_1\sin(\omega\tau_1).$$

We see that for $\omega \in (2(k-1)\pi/\tau_1, (2k-1)\pi/\tau_1)$, $a(\omega) < 0$ necessarily as $\sin(\omega\tau_1) > 0$ in these intervals and, by Lemma 2.5, $f_1(w) < 0$ when $\tau_1 < 1$. When $\sin(\omega\tau_1) > 0$ we rewrite $g(w) = (\tau_2 - \tau_1)\sin(\omega\tau_1) - \omega\tau_2$ and consider each branch individually. To do this, we must characterize what we call the distinct branches of the bifurcation set which we define in terms of branches of the arctangent function. For $0 < \tau_1 < \frac{\pi}{2}$ the *nth* branch of the bifurcation set ($n = 1, 2, 3, \ldots$) is given by

$$A = \sqrt{1 + \omega^2 - 2\omega\sin(\omega\tau_1)},$$

$$\tau_2 = \frac{1}{\omega}\operatorname{Arctan}\frac{\sin(\omega\tau_1) - \omega}{\cos(\omega\tau_1)} + \begin{cases} (2n-2)\frac{\pi}{\omega}, & \omega \in ((4k-3)\frac{\pi}{2\tau_1}, (4k-1)\frac{\pi}{2\tau_1}) \\ (2n-1)\frac{\pi}{\omega}, & \omega \in (0, \frac{\pi}{2\tau_1}) \cup ((4k-1)\frac{\pi}{2\tau_1}, (4k+1)\frac{\pi}{2\tau_1}) \end{cases}$$

where $k = 1, 2, \ldots$ and "Arctan" stands for the principal value of the inverse tangent function. On the *nth* branch, $\tau_2 > \tau_1$ for $\omega < (4n-3)\pi/2\tau_1$ and $\tau_2 < \tau_1$ thereafter. There are thus two cases to consider:

(i) $\omega \in ((2k-1)\pi/\tau_1, 2k\pi/\tau_1)$, $k = 1, 2, \ldots, n-1$. Here $(\tau_2 - \tau_1) > 0$, thus $(\tau_2 - \tau_1)\sin(\omega\tau_1) < 0$, and $a(\omega) < 0$ for ω in these intervals.

(ii) $\omega \in ((2k-1)\pi/\tau_1, 2k\pi/\tau_1)$, $k = n, \ldots$ Here $((\tau_2 - \tau_1)\sin(\omega\tau_1) - \omega\tau_2)_{\max} = \tau_1 - (2n-1)\pi/2$. Since $n > 1$, $(2n-1)\pi/2 > \pi/2 > 1$ and we conclude that $a(\omega) < 0$ for all ω in these intervals. □

We have analyzed in detail three explicit sets of parameter values: $\tau_1 = 0.65$, $\tau_1 = 1.5$ and $\tau_1 = 1.75$, the first of which satisfies the condition $\tau_1 < 1$ while the others do not. Evaluation of $a(\omega)$ shows that for the first set $a(\omega)$ is always negative (as Theorem 3.1 predicts !), while for the other two it changes from negative to positive at some value of ω.

Remark. Theorem 3.1 implies that for $\tau_1 < 1$, a Hopf bifurcation is supercritical at any point on the stability boundary. Although the theorem does not apply when $1 < \tau_1 < \pi/2$, it has been our observation that for τ_1 in this range the entire stability boundary is still supercritical, although the branches of the Hopf bifurcation set have parts where subcritical bifurcations would occur based on the sign of a in (3.21). This is illustrated by the dotted lines in Figs. 2.3 and 2.4.

3.2. Double Hopf. We now consider the situation where two branches of the stability boundary cross. At such points there are two values of ω satisfying (2.7) for the same values of A and τ_2:

$$\begin{aligned} A\cos(\omega_1\tau_2) &= -\cos(\omega_1\tau_1), & A\cos(\omega_2\tau_2) &= -\cos(\omega_2\tau_1), \\ A\sin(\omega_1\tau_2) &= \omega_1 - \sin(\omega_1\tau_1), & A\sin(\omega_2\tau_2) &= \omega_2 - \sin(\omega_2\tau_1). \end{aligned} \tag{3.22}$$

Correspondingly, there are two pairs of pure imaginary eigenvalues $\pm i\omega_1, \pm i\omega_2$. We can thus study, in a manner similar to that of the previous subsection, the four-dimensional centre manifold for (1.1) near these points. Once again we keep the discussion general, for arbitrary values of ω_1, ω_2. We note that much of the previous discussion may be generalized to this case by simply letting $\omega = \omega_1$ and $\omega = \omega_2$ in turn. The basis for the subspace P here is $\Phi = (\phi_1, \phi_2, \phi_3, \phi_4) = (\sin(\omega_1\theta), \cos(\omega_1\theta), \sin(\omega_2\theta), \cos(\omega_2\theta))$.

The basis for the adjoint problem, $\Psi = (\psi_1, \psi_2, \psi_3, \psi_4)^T$, is found as before with K now a (4×4) matrix given by

$$K = \begin{bmatrix} \frac{\langle \Phi_{12}^T, \Phi_{12} \rangle^T}{D_{12}^2} & 0 \\ 0 & \frac{\langle \Phi_{34}^T, \Phi_{34} \rangle^T}{D_{34}^2} \end{bmatrix}, \tag{3.23}$$

where

$$D_{ij}^2 = \det \langle \Phi_{ij}^T, \Phi_{ij} \rangle \quad \text{and} \quad \Phi_{ij} = (\phi_i, \phi_j).$$

The scalar products $\langle \phi_i, \phi_j \rangle$, $i, j = 1, 2$ are as in (3.14) with $\omega = \omega_1$, those for $\langle \phi_i, \phi_j \rangle$, $i, j = 3, 4$ are as in (3.14) with $\omega = \omega_2$, and the mixed terms $\langle \phi_i, \phi_j \rangle$, $i = 1, 2$, $j = 3, 4$, $\langle \phi_i, \phi_j \rangle$, $i = 3, 4$, $j = 1, 2$ are all zero.

The centre manifold will again be as in (3.4), with $\mathbf{z}$ satisfying the dynamical system of (3.5) but here

$$\mathbf{z} = (x, y, u, v)^T, \quad \Phi\mathbf{z} = \sin(\omega_1\theta)x + \cos(\omega_1\theta)y + \sin(\omega_2\theta)u + \cos(\omega_2\theta)v, \tag{3.24}$$

$$B = \begin{bmatrix} 0 & -\omega_1 & 0 & 0 \\ \omega_1 & 0 & 0 & 0 \\ 0 & 0 & 0 & -\omega_2 \\ 0 & 0 & \omega_2 & 0 \end{bmatrix}, \quad \mathbf{b} = \Psi(0) = \begin{pmatrix} K_{11}\phi_1(0) + K_{12}\phi_2(0) \\ K_{21}\phi_1(0) + K_{22}\phi_2(0) \\ K_{33}\phi_3(0) + K_{34}\phi_4(0) \\ K_{43}\phi_3(0) + K_{44}\phi_4(0) \end{pmatrix} = \begin{pmatrix} K_{12} \\ K_{22} \\ K_{34} \\ K_{44} \end{pmatrix}$$

and

$$\begin{aligned} f(\Phi z) &= \frac{1}{3}[-\sin(\omega_1\tau_1)x + \cos(\omega_1\tau_1)y - \sin(\omega_2\tau_1)u + \cos(\omega_2\tau_1)v]^3 \\ &\quad + \frac{A}{3}[-\sin(\omega_1\tau_2)x + \cos(\omega_1\tau_2)y - \sin(\omega_2\tau_2)u + \cos(\omega_2\tau_2)v]^3 \\ &= f_{111}x^3 + f_{112}x^2y + f_{113}x^2u + f_{114}x^2v + \cdots \\ &\quad \text{where e.g. } f_{111} = -\frac{1}{3}\left[\sin^3(\omega_1\tau_1) + A\sin^3(\omega_1\tau_2)\right]. \end{aligned} \tag{3.25}$$

Performing the substitutions as before leads to the following dynamical system:

$$\begin{aligned} \dot{x} &= -\omega_1 y + F^1_{111}x^3 + F^1_{112}x^2y + F^1_{113}x^2u + F^1_{114}x^2v + \cdots, \\ \dot{y} &= \omega_1 x + F^2_{111}x^3 + F^2_{112}x^2y + F^2_{113}x^2u + F^2_{114}x^2v + \cdots, \\ \dot{u} &= -\omega_2 v + F^3_{111}x^3 + F^3_{112}x^2y + F^1_{113}x^2u + F^3_{114}x^2v + \cdots, \\ \dot{v} &= \omega_2 u + F^4_{111}x^3 + F^4_{112}x^2y + F^2_{113}x^2u + F^4_{114}x^2v + \cdots, \end{aligned} \tag{3.26}$$

where $F^j_{111} = b_j f_{111}$, etc. The normal form for this system was calculated by Takens [17], to third order, to be

$$\begin{aligned} \dot{x}_1 &= [a_{11}r_1^2 + a_{12}r_2^2]x_1 - [\omega_1 + b_{11}r_1^2 + b_{12}r_2^2]y_1, \\ \dot{y}_1 &= [a_{11}r_1^2 + a_{12}r_2^2]y_1 + [\omega_1 + b_{11}r_1^2 + b_{12}r_2^2]x_1, \\ \dot{x}_2 &= [a_{21}r_1^2 + a_{22}r_2^2]x_2 - [\omega_2 + b_{21}r_1^2 + b_{22}r_2^2]y_2, \\ \dot{y}_2 &= [a_{21}r_1^2 + a_{22}r_2^2]y_2 + [\omega_2 + b_{21}r_1^2 + b_{22}r_2^2]x_2, \end{aligned} \tag{3.27}$$

where $r_j^2 = x_j^2 + y_j^2$. This can also be expressed in its polar form

$$\begin{aligned} \dot{r}_1 &= a_{11}r_1^3 + a_{12}r_1r_2^2, \\ \dot{r}_2 &= a_{21}r_1^2r_2 + a_{22}r_2^3, \\ \dot{\theta}_1 &= \omega_1 + b_{11}r_1^2 + b_{12}r_2^2, \\ \dot{\theta}_2 &= \omega_2 + b_{21}r_1^2 + b_{22}r_2^2, \end{aligned} \tag{3.28}$$

and its unfolding can be taken to be

$$\begin{aligned} \dot{r}_1 &= \mu_1 r_1 + a_{11}r_1^3 + a_{12}r_1r_2^2, \\ \dot{r}_2 &= \mu_2 r_2 + a_{21}r_1^2r_2 + a_{22}r_2^3, \\ \dot{\theta}_1 &= \omega_1 + b_{11}r_1^2 + b_{12}r_2^2, \\ \dot{\theta}_2 &= \omega_2 + b_{21}r_1^2 + b_{22}r_2^2. \end{aligned} \tag{3.29}$$

From our normal form calculations we find

$$a_{11} = \frac{1}{8}[3F^1_{111} + F^1_{122} + F^2_{112} + 3F^2_{222}], \tag{3.30}$$

$$a_{12} = \frac{1}{4}[F^1_{133} + F^1_{144} + F^2_{233} + F^2_{244}],$$

$$a_{21} = \frac{1}{4}[F^3_{113} + F^3_{223} + F^4_{114} + F^4_{224}],$$

$$a_{22} = \frac{1}{8}[3F^3_{333} + F^3_{344} + F^4_{334} + 3F^4_{444}].$$

Substituting in the values for the F^j gives

(3.31)

$$a_{11} = \frac{1}{8}\{-b_1[\sin(\omega_1\tau_1) + A\sin(\omega_1\tau_2)] + b_2[\cos(\omega_1\tau_1) + A\cos(\omega_1\tau_2)]\} = a_{12}/2,$$

$$a_{22} = \frac{1}{8}\{-b_3[\sin(\omega_2\tau_1) + A\sin(\omega_2\tau_2)] + b_4[\cos(\omega_2\tau_1) + A\cos(\omega_2\tau_2)]\} = a_{21}/2,$$

which can be reduced via (3.22), (3.24), and (3.23) to

$$a_{11} = -\frac{\psi_1(0)\omega_1}{8}, \qquad a_{22} = -\frac{\psi_3(0)\omega_2}{8}. \tag{3.32}$$

As indicated, $a_{12} = 2a_{11}$ and $a_{21} = 2a_{22}$; also a_{11} and a_{22} take the same value as a in the single Hopf calculations (see (3.21)), with $\omega = \omega_1$ and $\omega = \omega_2$, respectively. It is clear that those calculations yield all the information necessary to study the double Hopf point: in our case, the restrictions on the a_{ij} significantly reduce the possible behavior, but we still have to analyze (3.29).

The investigation of this four-dimensional system is greatly facilitated by noticing that, to second order, the azimuthal components have constant speed and that the radial components are independent of the azimuthal ones. It is thus natural to reduce the system to a two-dimensional one in the radial components. In this reduced system, a fixed point on one of the axis (either $r_1 = 0$ or $r_2 = 0$) corresponds to a limit cycle in the original system, a fixed point in the interior of the first quadrant corresponds to a two-dimensional torus, and a limit cycle corresponds to a three-dimensional torus in the original, four-dimensional system (3.29). Guckenheimer and Holmes [7] have shown that depending on the values of the cubic coefficients a_{ij}, there were 12 different cases possible as phase portraits of the unfolded system.

In the case $\tau_1 < 1$, Theorem 3.1 shows that $a(\omega) < 0$ on each branch for all ω, thus at each of the double bifurcation points we expect to have all the $a_{ij} < 0$. Using this and the relationship between a_{11}, a_{22} and a_{12}, a_{21} it is a simple matter to verify that the bifurcation diagram of the unfolding in this case is as pictured in Fig. 3.2, which is case Ib of Fig. 7.5.2 in [7], with a time reversal ($t \to -t$). In this illustration, different sectors in the plane of the unfolding parameters (μ_1, μ_2) give different phase portraits of the planar system in (r_1, r_2). This is the situation at all intersection points for the first set of parameter values considered in the previous section. If $\tau_1 > 1$ the situation will depend on how the double bifurcation points line up with the places where $a(\omega)$ is positive or negative. For the second set of parameter values considered, although $a(\omega) > 0$ on some region of the curves, the points of intersection correspond to points where $a(\omega) < 0$ on both curves. The unfolding is therefore the same as the previous set, i.e., that of Fig. 3.2. For the third set of parameter values, some of the double bifurcation points have $a_{11} > 0$ and $a_{22} < 0$, and thus the unfolding is as pictured in Fig. 3.3 (which is case VIa of Fig. 7.5.5 of [7]). Although it seems plausible that there should also exist double Hopf points at which both a_{ii} are positive, further numerical investigations have been futile in finding such points.

The unfoldings illustrated in Figs. 3.2 and 3.3 give us some insight into the dynamics of the full equations, which can be verified with numerical simulations at the

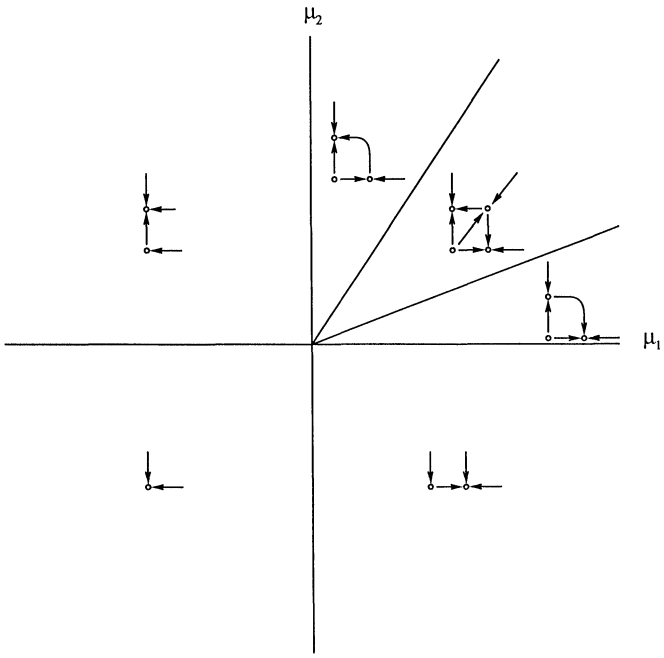

FIG. 3.2. *Bifurcation set of the unfolding from* (3.29): *according to the values of* μ_1 *and* μ_2 *in the different regions, the flow in the* r_1 *and* r_2 *plane is locally* (r_1 *and* r_2 *small*) *as shown. The case shown here is the interaction of two supercritical Hopf bifurcations, for example, at* $\tau_1 = 1.5$, *near* $A = 0.6$ *and* $\tau_2 = 5.3$.

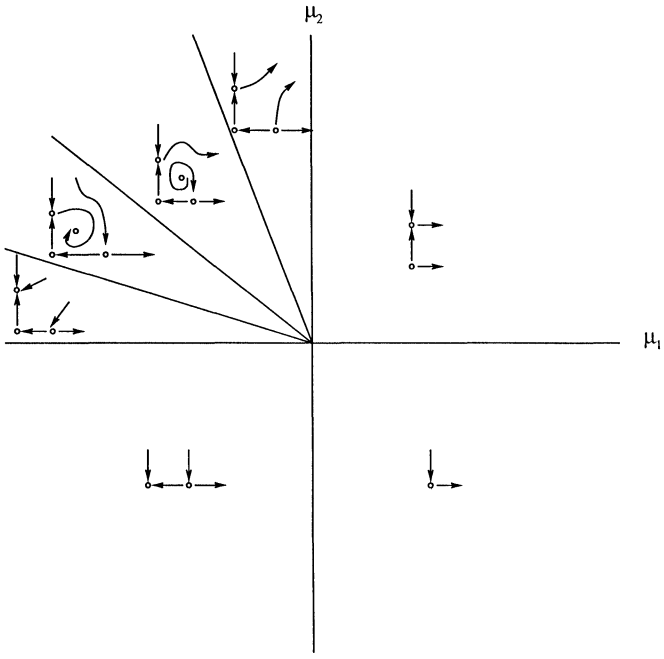

FIG. 3.3. *Same as in Fig.* 3.2, *except the case shown here is the interaction of a supercritical Hopf bifurcation with a subcritical Hopf bifurcation, for example at* $\tau_1 = 1.75$, *near* $A = 0.21$ *and* $\tau_2 = 12.5$.

appropriate parameter values. The beauty of these results is that we do not have to do extensive numerical simulations to find the "interesting" behavior, we already know where it exists. Two examples of simulations in such regions are shown in Figs. 3.4–3.5.

Figure 3.4 shows the results for $\tau_1 = 1.5$ near the supercritical-supercritical double Hopf interaction. The simulations were performed at the values $A = 0.61$ and $\tau_2 = 5.415$, which corresponds to the interior wedge region of the first quadrant in Fig. 3.2. Pictured are two sets of initial conditions: solutions from the first one go to a limit cycle (depicted in (a)), while solutions to the second one initially exhibit torus-like transient behavior (shown in (b)), but eventually approach another limit cycle (in (c)).

Results near the first supercritical-subcritical double Hopf point, at $\tau_1 = 1.75$ are shown in Fig. 3.5. The parameter values in (a) are $A = 0.20308$ and $\tau_2 = 12.543$, which correspond to values of μ_1 and μ_2 in the third quadrant in Fig. 3.3. Two different sets of initial conditions are used, the first one leading to a solution spiraling into the origin, the other one approaching a limit cycle. The parameter values for (b) and (c) correspond to the lowest interior wedge of the $\mu_1 < 0$ and $\mu_2 > 0$ quadrant in Fig. 3.3. Part (b) shows one initial condition which tends to a stable torus, and part (c) presents a different initial condition leading to a solution approaching a stable limit cycle. While this analysis may appear to be complete, it is clear from some of the numerical simulations that the unfoldings have not captured all of the dynamics. In the case of Fig. 3.4, the coexistence of a stable fixed point and a limit cycle is demonstrated, but the limit cycle was not expected from the unfolding. Furthermore, the supercritical-subcritical unfolding of Fig. 3.3 indicates that in a large region of parameter space near the double bifurcation point no attractor exists. This is clearly in conflict with our intuition about the solutions we expect for an equation modelling a physical situation, as well as numerical simulations we have done in such regions. This is not a failure of the method, but only an indication that we have reached the limits of its region of validity. In particular, for the parameter values used in Fig. 3.4, the cubic coefficients are quite small, and it calls into question our neglect of the "higher order" terms in the centre manifold and normal form calculations. Preliminary analysis has shown that many of these inadequacies can be dealt with by including the fifth order terms in our calculations and unfoldings. However, we leave discussion of the details of this analysis to a future paper.

4. Discussion. The local stability of (1.1) has been considered by a few authors in the past, and partial analysis performed in different notations. Our approach provides unique insight into the stability regions, in parameter space, and their dynamical evolution as one privileged parameter is altered. We now compare the results of the previous sections with some earlier and recent work.

In [16], Nussbaum considers the equation

$$z + \alpha e^{-z} + \beta e^{-\gamma z} = 0. \tag{4.1}$$

In the case $1 < \gamma \leq 2$, the author claims that the problem is equivalent to that of one delay via the following.

THEOREM 4.1 (Nussbaum [16]). *Let* $1 < \gamma \leq 2$. *Define* r *by* $(\alpha, \beta) = r(\sin\theta, \cos\theta)$, $0 \leq \theta \leq \pi/2$ *and* r_1 *by*

$$r_1(\theta, \gamma) = \frac{\nu_1}{\cos\theta \sin\nu_1 + \sin\theta \sin\gamma\nu_1},$$

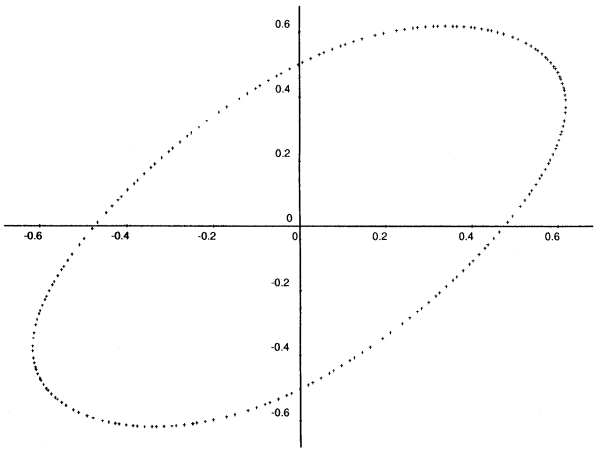

(a)

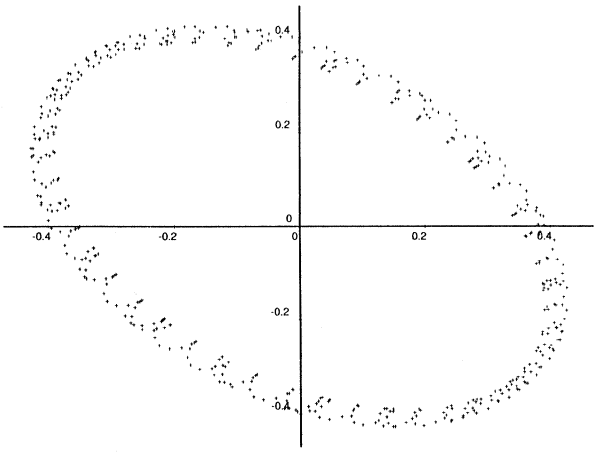

(b)

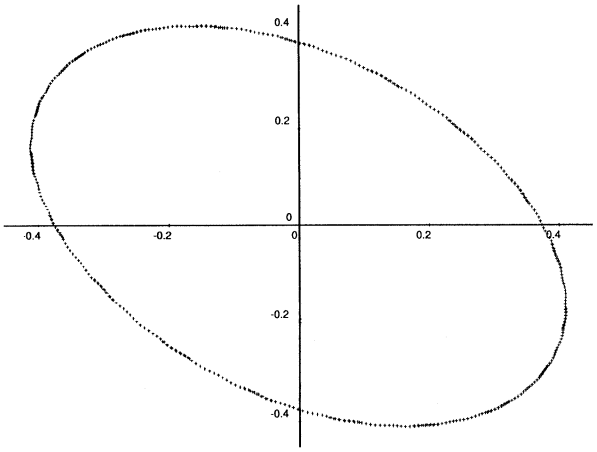

(c)

FIG. 3.4. *Numerical Simulations of* (1.1) *for* $\tau_1 = 1.5$, $\tau_2 = 5.415$, $A = 0.61$. (a) $x_1 = 1.0$, $x_2 = 0.0$, $t_f = 125$; (b) $x_1 = 0.0$, $x_2 = 1.0$, $t_f = 125$; (c) $x_1 = 0.0$, $x_2 = 1.0$, $t_f = 625$. *Points are displayed in the pseudophase plane* $(x(t - \tau_1), x(t))$.

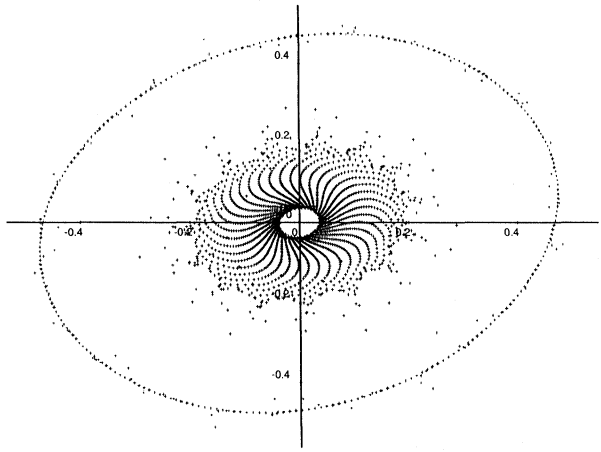

(a)

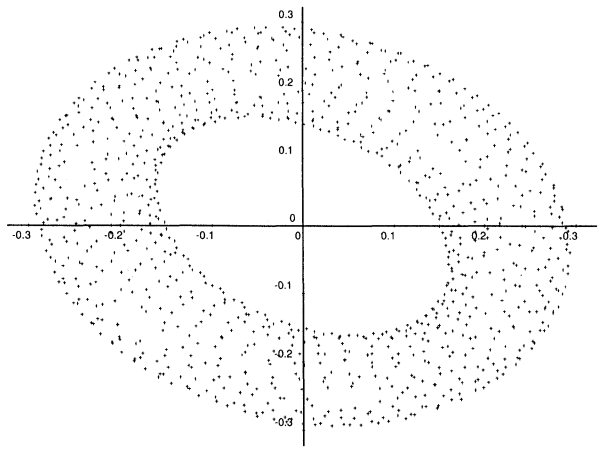

(b)

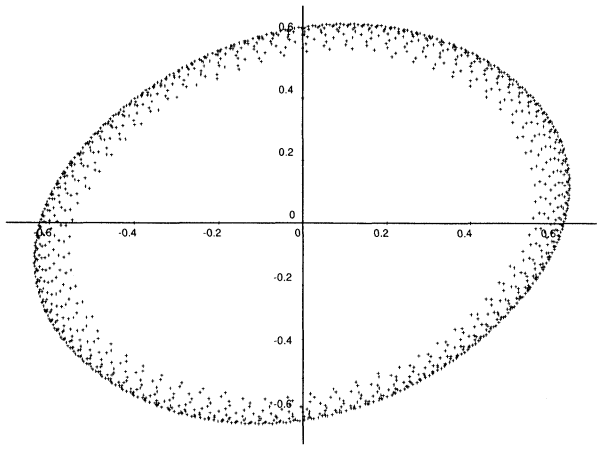

(c)

FIG. 3.5. *Numerical Simulations of* (1.1) *for* $\tau_1 = 1.75$. (a) $\tau_2 = 12.543$, $A = 0.20308$, $x_1 = 1.0$, $x_2 = 0.0$; $x_1 = 0.3$, $x_2 = 0$; (b) $\tau_2 = 12.600$, $A = .21583$,$x_1 = 0.4$, $x_2 = 0.0$; (c) τ_2 *and* A *same as in* (b), *but here* $x_1 = 0.6$, $x_2 = 0.0$. *Points are displayed in the pseudo-phase plane* $(x(t - \tau_1), x(t))$.

where $0 \leq \nu_1 \leq \pi/2$ *solves*

$$\cos\theta \cos\nu_1 + \sin\theta \cos\gamma\nu_1 = 0.$$

Consider only those solutions, z, such that $0 < \mathrm{Im}(z) < \pi$. *Then if* $r > r_1$ (4.1) *has precisely one such solution with positive real part, if* $r < r_1$ *it has no solution with positive real part, and if* $r = r_1$ *it has one such solution with zero real part.*

Comparing Nussbaum's rescaled variables with ours reveals the relationships

$$\gamma = \frac{\tau_2}{\tau_1} \quad \text{and} \quad r = \tau_1\sqrt{1+A^2}. \tag{4.2}$$

Thus the restriction $1 < \gamma \leq 2$ corresponds, on our stability diagrams (Figs. 2.1 to 2.4), to considering only a strip $\tau_1 < \tau_2 \leq 2\tau_1$. It is then easy to see why the author considers this case to be equivalent to the case of one delay. For, within this strip, there is only one curve of loss of stability as one increases A holding τ_1 fixed, or as one increases τ_1 holding A fixed. Nussbaum goes on to show that the case $\gamma > 2$ is, in his words, "considerably more complicated." Our analysis reveals and explains this phenomena. Although we have chosen a normalization of the coefficients such that our parameter plane contains one delay and one coefficient, we very clearly see that the value of the second, fixed, delay has a tremendous influence on the stability properties of (1.1): as one-dimensional paths are traversed in this parameter plane, the number of stability switches, if any, is highly dependent upon the value of this second delay, and, also, on the direction of this path.

More recently, Hale and Huang [11] have considered the stability of

$$\dot{x}(t) = -ax(t) - bx(t-r) - cx(t-\sigma) \tag{4.3}$$

in the $r - \sigma$ plane for various intervals in a, b, c. Their results may be compared with ours by taking $a = 0$, $b = 1$ and $c = A > 0$. Our studies thus fall into their cases IA ($c = A < 1$), IC ($c = A = 1$) and III (i) ($c = A > 1$). Comparison then shows that our results are consistent with theirs. However, their case IA does not show the situation of Fig. 2.3 where for $\tau_1 > \pi/2$ and $A < 1$ the trivial solution is unstable for $\tau_2 = 0$ and restabilizes for some larger values of τ_2. In fact, they conjectured that there is only one connected stable region (in the parameter plane of the two delays): our results seem to show that this is not always the case.

On the more practical side, Mizuno and Ikeda [15] have looked at the stability properties of

$$\gamma^{-1}\dot{\phi}(t) = -\phi(t) + \eta A[\phi(t-t_1) + \phi(t-t_2)] \tag{4.4}$$

to explain the results of some laser experiments. This equation is a version of (4.3) with the parameters restricted to $a = \gamma > 0$ and $b = c = \eta A$. They see changes in stability, and a structure on all scales which they analyze using number-theoretic methods (continued fractions, Farey series). Their approach is quite similar to that of Hale and Huang [11].

Also in the context of lasers, Grigorieva et al. [6] have studied the system of equations

$$\begin{aligned} \dot{u}(t) &= v[k(t) - 1 - \alpha u(t-\tau)]u(t) + vu_0, \\ \dot{k}(t) &= k_0 - k(t) - u(t)k(t), \end{aligned} \tag{4.5}$$

describing a single time delayed, negative feedback loop. Their diagrams in gain-delay (α-τ) space [ibid, Fig. 1] of the loss of stability of the steady states are clearly reminiscent of our stability plots (cf. Figs. 2.1 and 2.2).

Finally, Mahaffy et al. [14] have studied the equation

$$\dot{x}(t) = -A - Bx(t-1) - Cx(t-R) \tag{4.6}$$

in the three-dimensional (A, B, C) parameter space for different values of the delay ratio $0 < R \leq 1/2$. Since our equation is their case $A = 0$, a comparison is restricted to their Fig. 4.3. In this figure, a path along which B is constant and C increases, corresponds in our figures to a path where τ_1 is constant, $\tau_2 = \tau_1/3$ and A increases. This figure is consistent with our stability results, for example, the drastic change in the stability region at $\tau_1 = \pi/2$ in our figures is represented by the crossing of the first stability surface in their figure.

Each of the above works has filled in some "piece of the puzzle" of the two delay problem. We feel our approach is more transparent than most of the previous work, since we can obtain a "piecewise global" perception of the bifurcation picture. In addition, we have studied not only the linear stability of the trivial solution, but also the criticality of the Hopf bifurcation occurring at its loss of stability: this consideration of nonlinear elements is essential to understand the appearance of such dynamically sophisticated elements as tori. Finally, we have considered in detail the possible solutions resulting from the double Hopf points.

Acknowledgments. The authors have benefitted from conversations with A. Beuter, L. Glass, J. Mahaffy, M. Mackey and J. Milton, as well as a meticulous reading of the manuscript by a referee. Part of this work was done during a visit to the Fields Institute for Research in Mathematical Sciences (Waterloo), whose staff and officers are thanked for their hospitality.

REFERENCES

[1] J. Bélair and M. Mackey, *Consumer memory and price fluctuations in commodity markets: An integrodifferential model*, J. Dynamics Differential Equations, 1 (1989), pp. 299–325.

[2] A. Beuter, J. Bélair, and C. Labrie, *Feedback and delays in neurological diseases: a modeling study using dynamical systems*, Bull. Math. Biol., 55 (1993), pp. 525–541.

[3] A. Beuter, D. Larocque, and L. Glass, *Complex oscillations in a human motor system*, J. Motor Behaviour, 21 (1989), pp. 277–289.

[4] S. Campbell and J. Bélair, *Analytical and symbolically-assisted investigation of Hopf bifurcations in delay-differential equations*, preprint, 1993.

[5] K. Cooke and Z. Grossman, *Discrete delay, distributed delay and stability switches*, J. Math. Anal. Appl., 86 (1982), pp. 592–627.

[6] E. Grigorieva, S. Kashchenko, N. Loiko, and A. Samson, *Nonlinear dynamics in a laser with a negative delayed feedback*, Physica D, 59 (1992), pp. 297–319.

[7] J. Guckenheimer and P. Holmes, *Nonlinear Oscillations, Dynamical Systems and Bifurcations of Vector Fields*, Springer-Verlag, New York, 1983.

[8] J. Hale, *Functional Differential Equations*, Springer, Berlin, 1977.

[9] ———, *Nonlinear oscillations in equations with delays*, in Nonlinear Oscillations in Biology, K. Hoppenstadt, ed., American Mathematical Society, Providence, RI, 1979.

[10] ———, *Flows on center manifolds for scalar functional differential equations*, Proc. Roy. Soc. Edinburgh, 101A (1985), pp. 193–201.

[11] J. Hale and W. Huang, *Global geometry of the stable regions for two delay differential equations*, J. Math. Anal. Appl., 178 (1993), pp. 344–362.

[12] N. Hayes, *Roots of the transcendental equation associated with a certain difference-differential equation*, J. London Math. Soc., 25 (1950), pp. 226–232.

[13] V. Kolmanovskii and V. Nosov, *Stability of functional differential equations*, in Mathematics in Science and Engineering, vol. 180, Academic Press, New York, 1986.

[14] J. Mahaffy, P. Zak, and K. Joiner, *A Geometric Analysis of the Stability Regions for a Linear Differential Equation with Two Delays*, preprint, 1992.
[15] M. Mizuno and K. Ikeda, *An unstable mode selection rule: frustrated optical instability due to two competing boundary conditions*, Physica D, 36 (1989), pp. 327–342.
[16] R. Nussbaum, *Differential delay equations with two time lags*, Mem. Amer. Math. Soc., 16 (1975), pp. 1–62.
[17] F. Takens, *Singularities of vector fields*, Publications Mathématiques de l'IHES, 43 (1974), pp. 47–100.
[18] Waterloo Maple Software, *Maple V*, University of Waterloo, Waterloo, Canada, 1990.